https://doi.org/10.1093/plphys/kiad021 PLANT PHYSIOLOGY 2023: 00: 1–14

Plant Physiology®

Research Article

The flowering time regulator FLK controls pathogen defense in *Arabidopsis thaliana*

Matthew Fabian [1,†] **Min Gao** [1,2,†‡] **Xiao-Ning Zhang** [2] **Jiangli Shi** [1,3,§] **Leah Vrydagh** [1] **Sung-Ha Kim** [3] **Priyank Patel** [1] **Anna R. Hu** [2] **and Hua Lu** [1,*]

1 Department of Biological Sciences, University of Maryland Baltimore County, 1000 Hilltop Circle, Baltimore, Maryland 21250, USA
2 Biochemistry Program, Department of Biology, St Bonaventure University, St Bonaventure, New York 14778, USA
3 Department of Biology Education, Korea National University of Education, Chungbuk 28644, Korea

*Author for correspondence: hualu@umbc.edu (H.L)
†These authors contributed equally to this research.
‡Present address: State Key Laboratory of Crop Stress Biology in Arid Areas, College of Horticulture, Key Laboratory of Horticultural Plant Biology and Germplasm Innovation in Northwest China, Ministry of Agriculture, Northwest A&F University, Yangling, Shaanxi 712100, China.
§Present address: College of Horticulture, Henan Agricultural University, Zhengzhou 450002, China.

M.F. performed pathogen infections and PTI and ROS-related assays, measured flowering time and pathogen-induced SA accumulation, and assisted in the bioinformatics analysis. M.G. performed cell death staining, SA measurement, and gene expression analysis with the *flk* mutants and prepared samples for the RNA-seq experiments. J.S. assisted in the cloning of the *FLK* gene. X.Z. cloned the *FLK-GFP* construct and conducted plant transformation and confocal microscopy for FLK-GFP localization. L.V. did RT-PCR for detection of *ACD6* isoforms and RT-qPCR for expression of *FLC*, *PDF1.2*, and ACD6 isoforms. S.K. measured flowering time. P.P. assisted M.F. in PTI assays. A.H. assisted in the bioinformatics analysis. H.L. designed experiments, conducted genetic crosses, analyzed gene alternative splicing, and wrote the manuscript with input from all authors.
The author responsible for distribution of materials integral to the findings presented in this article in accordance with the policy described in the Instructions for Authors (https://academic.oup.com/plphys/pages/General-Instructions) is: Hua Lu (hualu@umbc.edu).

Abstract

Plant disease resistance is a complex process that is maintained in an intricate balance with development. Increasing evidence indicates the importance of posttranscriptional regulation of plant defense by RNA binding proteins. In a genetic screen for suppressors of Arabidopsis (*Arabidopsis thaliana*) *accelerated cell death 6-1* (*acd6-1*), a small constitutive defense mutant whose defense level is grossly in a reverse proportion to plant size, we identified an allele of the canonical flowering regulatory gene *FLOWERING LOCUS K HOMOLOGY DOMAIN* (*FLK*) encoding a putative protein with triple K homology (KH) repeats. The KH repeat is an ancient RNA binding motif found in proteins from diverse organisms. The relevance of KH-domain proteins in pathogen resistance is largely unexplored. In addition to late flowering, the *flk* mutants exhibited decreased resistance to the bacterial pathogen *Pseudomonas syringae* and increased resistance to the necrotrophic fungal pathogen *Botrytis cinerea*. We further found that the *flk* mutations compromised basal defense and defense signaling mediated by salicylic acid (SA). Mutant analysis revealed complex genetic interactions between *FLK* and several major SA pathway genes. RNA-seq data showed that *FLK* regulates expression abundance of some major defense- and development-related genes as well as alternative splicing of a number of genes. Among the genes affected by *FLK* is *ACD6*, whose transcripts had increased intron retentions influenced by the *flk* mutations. Thus, this study provides mechanistic support for *flk* suppression of *acd6-1* and establishes that *FLK* is a multifunctional gene involved in regulating pathogen defense and development of plants.

Received July 22, 2022. Accepted December 18, 2022. Advance access publication January 20, 2023

Introduction

Plants are constantly challenged by a myriad of pathogens with various lifestyles. In response, plants can recognize many pathogen-derived molecules, such as pathogen associated molecular patterns (PAMPs) and effector proteins, and subsequently activate layers of defense responses, including PAMP-triggered immunity (PTI), effector-triggered immunity, and systemic acquired resistance (Boller and Felix, 2009; Dodds and Rathjen, 2010; Fu and Dong, 2013; Toruno et al., 2016). Depending on the type of invading pathogen, plants deploy different and sometimes conflicting downstream signaling to combat the invader. Salicylic acid (SA) is generally considered to be important for defense against biotrophic pathogens, e.g. *Pseudomonas syringae*. The major SA biosynthesis genes include *ISOCHORISMATE SYNTHASE 1* (*ICS1*) and *HOPW1-1-INTERACTING3* (*WIN3*) (Wildermuth et al., 2001; Lee et al., 2007; Rekhter et al., 2019). Additional genes, such as *ACCELERATED CELL DEATH 6 (ACD6)*, *ENHANCED DISEASE SUSCEPTIBILITY* (*EDS1*), and *PHYTOALEXIN-DEFICIENT 4* (*PAD4*) (Falk et al., 1999; Lu et al., 2003), also affect SA levels but their functions have not been completely understood. SA receptors *NONEXPRESSER OF PR GENES 1* (*NPR1*), *NPR3*, and *NPR4* perceive and transduce SA signal to the nucleus for reprogramming gene expression (Wu et al., 2012; Yan and Dong, 2014). On the other hand, jasmonic acid (JA) promotes resistance to necrotrophic pathogens, e.g. *Botrytis cinerea*, as well as to insects (Glazebrook, 2005; Campos et al., 2014). SA and JA act antagonistically in the defense response against certain pathogens, yet they also work synergistically under other stress conditions. Proper interplay between signaling pathways is important to ensure robust plant defense. Without a thorough understanding of how different signaling molecules activate defense against pathogens, our design of strategies to improve disease resistance of crop plants against their natural pathogens will be limited.

Defense is an energetically costly process and defense activation against some pathogens can come at the expense of plant development (Karasov et al., 2017; Ning et al., 2017). Flowering is one of the most critical developmental landmarks in the lifecycle of plants. It is well known that flowering in the model plant Arabidopsis (*Arabidopsis thaliana*) is tightly controlled by at least five pathways: the autonomous pathway, photoperiod (light), vernalization, hormones, and the circadian clock (Amasino, 2010). These pathways ultimately converge upon a few downstream genes, e.g. the flowering repressor gene *FLOWERING LOCUS C* (*FLC*) and flowering activator genes *FLOWERING LOCUS T* and *SUPPRESSOR OF OVEREXPRESSION OF CONSTANS1*, to determine flowering time. Growing evidence supports the involvement of flowering pathways in Arabidopsis defense, including the autonomous pathway genes *FPA* and *FLOWERING LOCUS D* (Lyons et al., 2013; Singh et al., 2013), certain light receptors (Genoud et al., 2002; Griebel and Zeier, 2008; Roden and Ingle, 2009), flowering regulatory hormones (Spoel and Dong, 2008; Bari and Jones, 2009), and the circadian clock (Lu et al., 2017). On the other hand, defense activation reciprocally affects flowering. For instance, pathogen infection (Korves and Bergelson, 2003) and changes in SA levels via exogenous SA application or genetic manipulation, i.e. using SA mutants *ics1* and *eds5*, are associated with altered flowering time (Martinez et al., 2004; Jin et al., 2008; March-Diaz et al., 2008; Endo et al., 2009; Wada et al., 2009; Liu et al., 2012). These observations suggest crosstalk between plant defense and flowering control. Mechanisms underlying this crosstalk remain to be fully elucidated.

The *FLOWERING LOCUS K HOMOLOGY DOMAIN* (*FLK*) gene is known as a positive regulator of flowering, acting in the autonomous pathway. It encodes a putative protein with three K homology (KH) repeats (Lim et al., 2004; Mockler et al., 2004). The KH domain is an ancient RNA binding motif found in proteins from diverse organisms (Nicastro et al., 2015). The KH domain has about 70 amino acids and can be in arrays of up to 15 KH repeats. Some KH-domain proteins were shown to function in RNA metabolism, affecting pre-mRNA processing and mRNA stability. Disruptions of KH-domain proteins are associated with multiple diseases in humans (Geuens et al., 2016). There are 26 predicted KH-domain proteins in Arabidopsis (Lorkovic and Barta, 2002) but only a few of them have been characterized. Like FLK, several Arabidopsis KH-domain proteins were shown to play roles in flowering control (Cheng et al., 2003; Ripoll et al., 2009; Yan et al., 2017; Ortuno-Miquel et al., 2019; Woloszynska et al., 2019). Some KH-domain proteins were shown to be important for stress response, including resistance against a fungal pathogen (Thatcher et al., 2015) and abiotic stress (Chen et al., 2013; Guan et al., 2013). To date, none of the KH-domain proteins are shown to influence both defense and development.

To better understand gene networks involved in pathogen defense, we have utilized the Arabidopsis mutant *accelerated cell death6-1* (*acd6-1*) in our studies. *acd6-1* exhibits a constitutively high level of defense that is inversely associated with the size of the plant (Rate et al., 1999; Lu et al., 2003). This feature of *acd6-1* makes it a convenient genetic tool in gauging genetic interactions among defense genes (Song et al., 2004; Ng et al., 2011; Wang et al., 2011a; Wang et al., 2014; Hamdoun et al., 2016; Zhang et al., 2019). *acd6-1* has also been proven as a powerful starting material in a large-scale genetic screen for *acd6-1* suppressors, allowing for the uncovering of defense genes (Lu et al., 2009; Wang et al., 2014). From this genetic screen, we isolated an allele of the *FLK* gene, *flk-5*, that suppressed *acd6-1*-conferred phenotypes, including SA accumulation, cell death, and dwarfism. In addition to late flowering, *flk* mutants showed enhanced susceptibility to the biotrophic pathogen *Pseudomonas syringae* but enhanced resistance to the necrotrophic pathogen *Botrytis cinerea*. In addition, the *flk* mutants exhibited compromised SA accumulation and basal defense upon *P. syringae* infection and/or elicitation by *P. syringae* derived molecules. RNA-seq analysis revealed that expression of

some major defense- and development-related genes as well as alternative splicing of a number of genes were influenced by the *flk* mutations. We further provided evidence to show that the *ACD6* gene is a potential target of FLK for alternative splicing. Together our data support that FLK is a multifunctional protein important for plant defense and development and establish mechanistic links for these roles of FLK.

Results

Identification of an *FLK* allele from *acd6-1* suppressor screen

In order to better understand defense gene networks, we took advantage of the Arabidopsis mutant *acd6-1* whose defense level is in a gross inverse association with the size of the plant (Rate et al., 1999; Lu et al., 2003). We conducted a large-scale screen of an *acd6-1* mutant library generated by T-DNA insertional mutagenesis for *acd6-1* suppressors, which showed partially increased plant size and were likely disrupted in genes involved in pathogen defense (Lu et al., 2009; Wang et al., 2014). Among the suppressor mutants isolated, we identified a plant displaying delayed flowering time. We backcrossed the mutant to *acd6-1* two times and confirmed the association of *acd6-1* suppression and late flowering phenotypes. In addition, we outcrossed the suppressor mutant to Arabidopsis Col-0 and obtained the single mutant. We further conducted TAIL-PCR (Liu et al., 1995) and located a T-DNA insertion in the second intron of the *FLK* gene (Figure 1A). *FLK* encodes a protein with three predicted KH repeats that is previously known as a flowering regulator acting in the autonomous pathway (Lim et al., 2004; Mockler et al., 2004). Because four other *flk* mutants were previously described (Lim et al., 2004; Mockler et al., 2004), we designated this allele as *flk-5*. The *acd6-1 flk-5* mutant showed a partial suppression of *acd6-1* in terms of plant size and cell death, and it flowered later than both the *acd6-1* mutant and Col-0 (Figure 1, B–D). Such partial suppression of *acd6-1*-conferred phenotypes was confirmed by introducing another *FLK* allele, *flk-1* (SALK_007750), into *acd6-1* (Figure 1). In addition, we made a construct carrying the 2.3 kb *FLK* promoter and the full-length *FLK* genomic fragment that was translationally fused with the reporter gene *GFP* (*FLK-GFP*) and used it to transform *flk-1*. Independent homozygous *FLK-GFP*/*flk-1* transformants demonstrated a rescue of late flowering conferred by *flk-1* (Supplemental Figure S1, A and B). The FLK-GFP protein was localized to the nucleus (Supplemental Figure S1C).

FLK is a positive regulator of *P. syringae* resistance and a negative regulator of *B. cinerea* resistance

The suppression of *acd6-1*-conferred phenotypes by *flk* mutants suggests that FLK is important for pathogen defense, in particular with a role in SA regulation. To test this, we infected Col-0, *flk-1*, and *flk-5* plants with the virulent

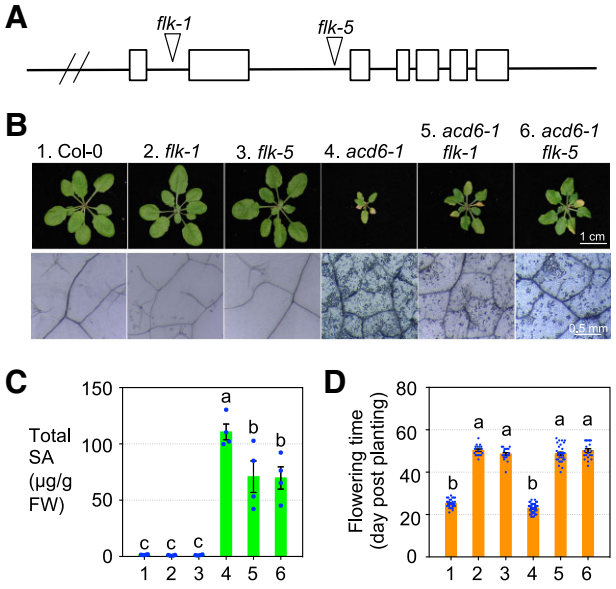

Figure 1 Mutations in *FLK* suppress *acd6-1*-conferred phenotypes and lead to late flowering. A, Gene structure of *FLK*. Triangles indicate the positions of two *FLK* alleles, boxes indicate exons, and the line indicates the promoter, introns, and 3′ downstream region. B, Pictures of 25-d old plants (upper panel) and cell death (lower panel). Leaves at the fourth to seventh positions of each genotype were stained with trypan blue for cell death. C, Salicylic acid (SA) quantification. Total SA was extracted from the plants and quantified by HPLC. D, Flowering time measurement. Plants were grown in a light cycle of 16 h L/8 h D and recorded for flowering time, days after planting for the first visible appearance of inflorescence of a plant. Error bars represent mean ± SEM in (C) ($n = 4$) and (D) ($n \geq 18$). Different letters in C and D indicate significant difference among the samples ($P < 0.05$; One-way ANOVA with post hoc Tukey's HSD test). These experiments were repeated two times with similar results.

P. syringae pv. *maculicola* ES4326 strain DG3 (*Pma*DG3). We found that both *flk* mutants were more susceptible than Col-0 and this susceptibility was rescued by *FLK-GFP*, as demonstrated in two representative rescued lines #7 and #20 (Figure 2A). The *flk* mutants also had lower SA accumulation and lower expression of the SA marker gene *PR1* than Col-0 with *Pma*DG3 infection (Figure 2, B and C), supporting the SA regulatory role of FLK.

Plant perception of biotrophic pathogens is often associated with activation of PTI, a basal level of defense (Zipfel et al., 2004). Flg22, a 22-aa peptide from the conserved region of the flagellin protein of *P. syringae*, is widely used to elicit PTI, including rapid oxidative burst, cell wall strengthening via callose deposition, and reduced plant growth. Within minutes of flg22 treatment, Col-0 and the two rescued lines activated an oxidative burst, producing a high level of ROS (Figure 2D, left). The *flk* mutations compromised such a ROS burst. This phenotype was further corroborated with another PAMP molecule, elf26, a 26-aa peptide from the elongation factor Tu protein (Kunze et al., 2004)

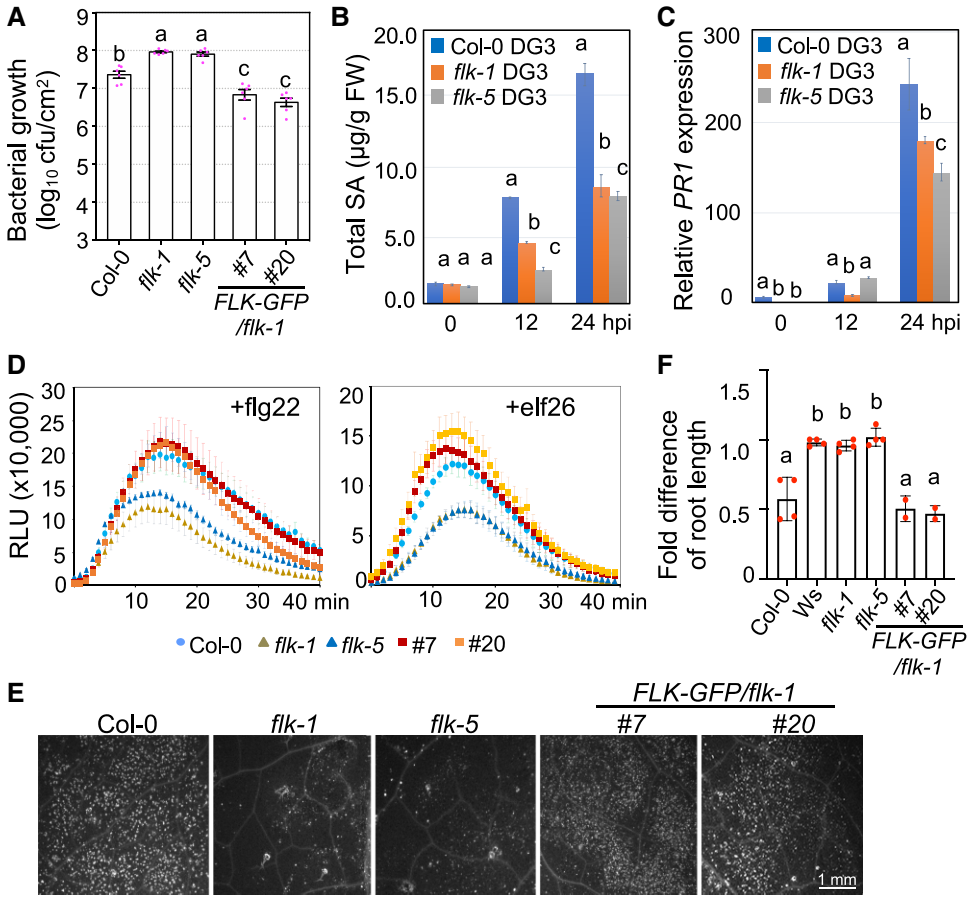

Figure 2 *FLK* positively regulates *P. syringae* resistance, salicylic acid (SA) accumulation, and PTI. A, Bacterial growth with *PmaDG3* infection ($n = 6$). B, Salicylic acid (SA) quantification with *PmaDG3* infection ($n = 2$). C, Expression of *PR1* with *PmaDG3* infection ($n = 3$). D, ROS burst in seedlings treated with 1 µM flg22 (left) and 1 µM elf26 (right) ($n = 12$). RLU: relative luminescence unit. E, Images of callose deposition. The fourth to seventh leaves of 25-d old plants were infiltrated with 1 µM flg22 for 24 h followed by callose staining, using 0.01% aniline blue. F, Root growth inhibition with 1 µM flg22 treatment. 4-d old seedlings were treated with 1 µM flg22 and measured for root length 4 d post treatment. The flg22-insensitive ecotype Ws that contains a loss-of-function mutation in the *FLS2* gene was included as a control. The fold difference is the ratio of flg22-treated and water-treated root length of each genotype. Data represent the average of three independent experiments. Error bars represent mean ± SEM in A, D, and F and mean ± STDV in panel B and C. Different letters indicate significant difference among the samples of the same time point ($P < 0.05$; One-way ANOVA with post hoc Tukey's HSD test). These experiments were repeated two times with similar results.

(Figure 2D, right). We also found that the *flk* mutants displayed fewer callose depositions and less seedling growth inhibition upon flg22 treatment (Figure 2, E and F). These *flk*-conferred PTI phenotypes were rescued by *FLK-GFP* (Figure 2, D–F). Together our data suggest that FLK positively regulates *P. syringae* resistance through activating SA signaling and PTI.

While SA is important for *P. syringae* resistance, SA could antagonize other signaling pathways to suppress plant defense against necrotrophic pathogens (Glazebrook, 2005; Campos et al., 2014). To test if this is a possibility in FLK-mediated defense, we infected the plants with the necrotrophic fungal pathogen *B. cinerea*. Compared with Col-0 and the two rescued lines, the *flk* mutants were more resistant to *B. cinerea* (Figure 3). Thus, this result supports a negative role of FLK in *B. cinerea* defense, likely through SA cross-talking with other defense signaling.

RNA-seq analysis supports the roles of FLK in defense and development regulation

To elucidate how FLK is mechanistically linked to plant defense and development, we performed RNA-seq analysis. We generated transcriptome profiles of Col-0, *flk-1*, *flk-5*, *acd6-1*, *acd6-1 flk-1*, and *acd6-1 flk-5*, using the Illumina NovaSeq 6000 platform. Principal component analysis of the sequencing data after removing low-quality reads showed an association of gene expression profiles of the replicates in each genotype (Figure 4A). To identify *FLK*-affected genes, we compared four groups: (a) Col-0 vs. *flk-1*; (b) Col-0 vs. *flk-5*; (c) *acd6-1* vs. *acd6-1 flk-1*; and (d) *acd6-1* vs. *acd6-1 flk-5*. We found that there was a total of 8,083 differentially expressed genes (DEGs) in at least one comparison group (adjusted p-value < 0.05) (Supplemental Dataset S1). Consistent with the known role of FLK in regulating development, Gene Ontology (GO) analyses showed

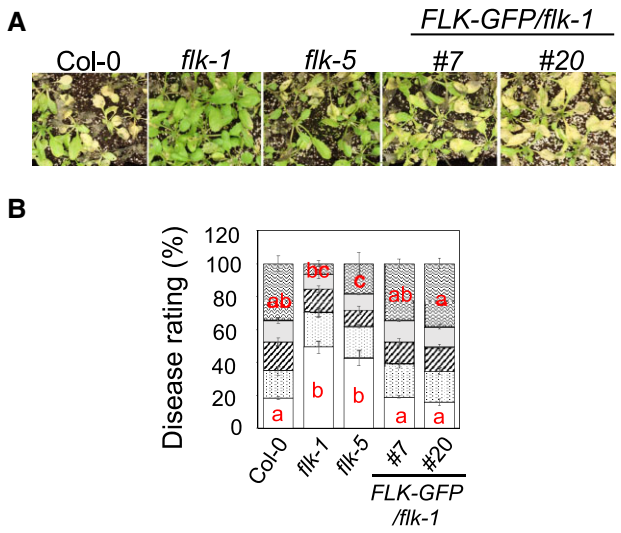

Figure 3 *FLK* negatively regulates *Botrytis* resistance. A, Pictures of *B. cinerea*-infected plants. B, Disease symptom scoring with *B. cinerea* infection. The rating scale is from 1 (bottom; no lesion or small, rare lesions) to 5 (top; lesions on over 70% of a leaf). Error bars represent mean ± SEM ($n = 30$). Different letters indicate significant difference among the samples in the same rating group ($P < 0.05$; One-way ANOVA with post hoc Tukey's HSD test). These experiments were repeated two times with similar results.

that the DEGs were significantly enriched in those involved in primary metabolism (GO:0009415 and GO:0010243) and development-related processes (GO:0009639 and GO:0048511) (Figure 4B). The flowering repressor gene *FLC* is among the development-related DEGs affected by the *flk* mutations. Expression of *FLC* was induced by *flk* mutations, which was validated by reverse transcription quantitative PCR (RT-qPCR) analysis (Supplemental Figure S2).

In addition, the DEGs affected by the *flk* mutations are enriched in those related to biotic and abiotic responses (GO:0009620 [response to fungus], GO:0009617 [response to bacterium], GO:0006979 [response to oxidative stress], GO:0010200 [response to chitin], GO:0009409 [response to cold], and GO:0009611 [response to wounding]) (Figure 4B). A total of 955 defense genes showed differential expression in at least one comparison group (Figure 4C and Supplemental Dataset S1). Defense genes affected by *flk* mutants are from multiple signal pathways involving SA, JA, ethylene (ET), programmed cell death (PCD), and/or PTI (Figure 4, C and D). Expression of most of these defense genes was suppressed by the *flk* mutations in the *acd6-1* background. For instance, several major SA pathway genes, including the major SA biosynthesis genes (*ICS1*/*EDS16* and *WIN3*/*AVRPPHB SUSCEPTIBLE 3* [Wildermuth et al., 2001; Lee et al., 2007; Rekhter et al., 2019], SA regulatory genes (*EDS1*, *PAD4*, *SENESCENCE-ASSOCIATED GENE101*, *CALMODULIN BINDING PROTEIN 60 g*, and *SYSTEMIC ACQUIRED RESISTANCE DEFICIENT 1*) (Feys et al., 2001, 2005; Wang et al., 2009; Zhang et al., 2010c; Wang et al., 2011b), and SA receptors (*NPR1* and *NPR3*) (Fu et al., 2012), showed lower expression in the *acd6-1 flk* mutants than in *acd6-1* (Figure 4D and Supplemental Dataset S1). This lower expression of SA pathway genes in the *acd6-1 flk* mutants is consistent with the suppression of *acd6-1*-conferred phenotypes in these plants, lending strong support for the role of FLK in SA regulation.

In the JA pathway, we found that a number of genes involved in JA biosynthesis showed reduced expression in *acd6-1 flk-1* and *acd6-1 flk-5*, compared with in *acd6-1* (Figure 4D and Supplemental Dataset S1). These JA genes include the *LIPOXYGENASE* genes (Vellosillo et al., 2007; Seltmann et al., 2010), *ALLENE OXIDE CYCLASE* (Hofmann and Pollmann, 2008), and the *12-oxophytodienoate reductase* genes (Schaller et al., 2000; Stintzi and Browse, 2000). No expressional changes were observed for the JA receptor gene *CORONATINE INSENSITIVE 1*, the key downstream signal transducer (transcription factor *MYELOCYTOMATOSIS* [*MYC2*]), and several *MYC2* target genes, including *NAC DOMAIN CONTAINING PROTEIN 19*, *ANAC055*, and *RESPONSIVE TO DESICCATION 26* (Bu et al., 2008; Zheng et al., 2012). However, we found that expression of several *JASMONATE ZIM-DOMAIN* genes (Vanholme et al., 2007) was suppressed while the JA signaling marker gene *PLANT DEFENSIN 1.2* (*PDF1.2*) was highly induced in the *acd6-1 flk* mutants compared with in *acd6-1*. Expression of *PDF1.2* was validated by RT-qPCR (Supplemental Figure S2). It is possible that at least some branches of JA signaling are affected by the *flk* mutations.

Additionally, we observed a down-regulation of key PTI-related genes in the *acd6-1 flk* mutants compared with in *acd6-1*. These PTI genes include the pattern recognition receptors (*FLAGELLIN-SENSING2* and *ELONGATION FACTOR-TU RECEPTOR*), the coreceptor *BRASSINOSTEROID INSENSITIVE 1-ASSOCIATED RECEPTOR KINASE* [Boller and Felix, 2009], PTI signal transducers (*MITOGEN-ACTIVATED PROTEIN KINASE 3*, *MITOGEN-ACTIVATED PROTEIN KINASE KINASE 5*, and a number of WRKY genes [e.g. *WRKY22*, *WRKY* 29, and *WRKY* 33]) (Asai et al., 2002; Hsu et al., 2013), and members of the *Arabidopsis Tóxicos en Levadura* gene family that were shown early responses to PTI (Libault et al., 2007; Lin et al., 2008). These data strongly support the role of FLK in PTI regulation.

FLK plays a role in alternative splicing

Some KH-domain proteins were shown to function in RNA metabolism (Nicastro et al., 2015). For instance, two of the most similar human homologs of FLK, the POLY(C)-BINDING PROTEIN and NOVA ALTERNATIVE SPLICING REGULATOR 1 proteins, were shown to regulate RNA alternative splicing (Zhang et al., 2010a, 2010b). To test a potential role of FLK in RNA alternative splicing, we analyzed the differential alternative splicing (DAS) profile, using the RNA-seq data. We found that there was a total of 867 DAS genes significantly influenced by the *flk* mutations in at least one of these comparison groups: (a) Col-0

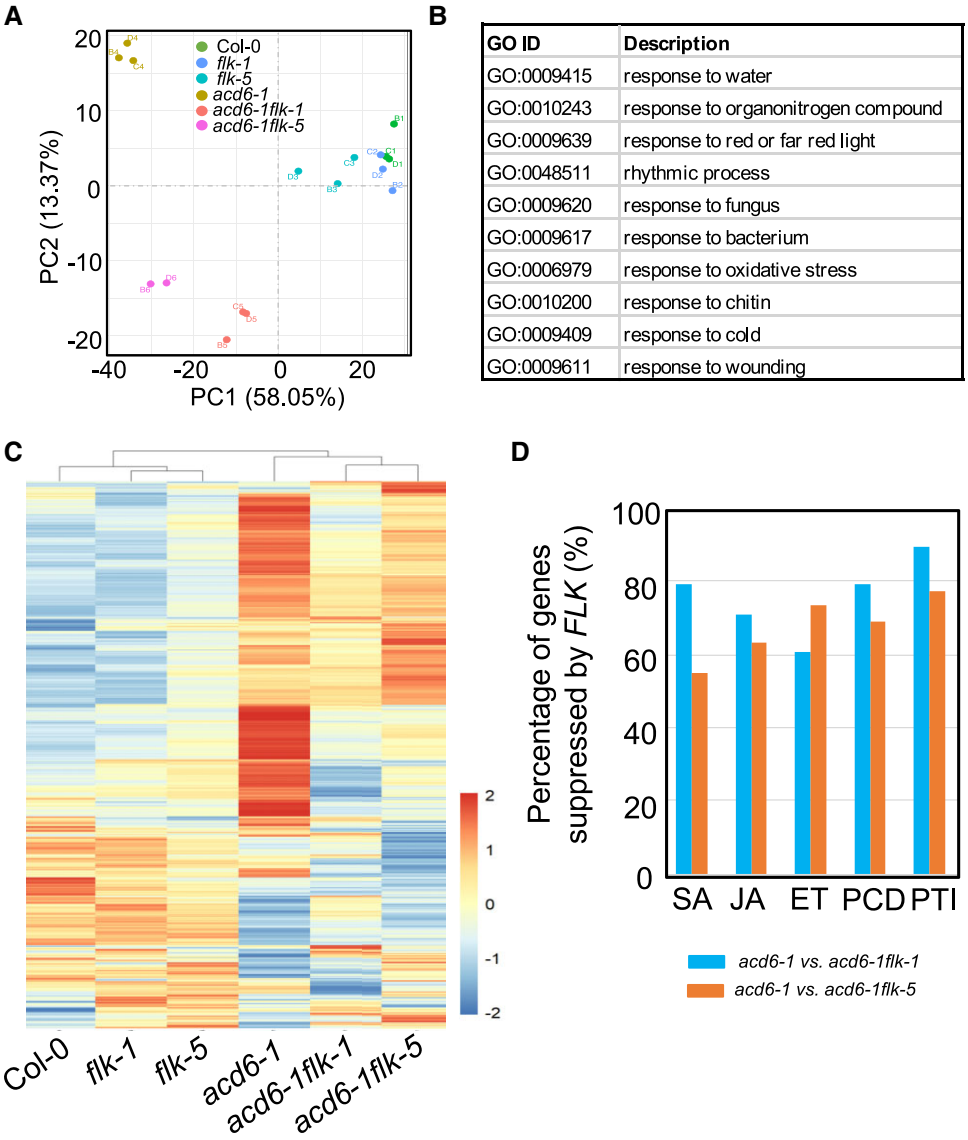

GO ID	Description
GO:0009415	response to water
GO:0010243	response to organonitrogen compound
GO:0009639	response to red or far red light
GO:0048511	rhythmic process
GO:0009620	response to fungus
GO:0009617	response to bacterium
GO:0006979	response to oxidative stress
GO:0010200	response to chitin
GO:0009409	response to cold
GO:0009611	response to wounding

Figure 4 RNA-seq analysis reveals genes differentially affected by the *flk* mutations. A, Principal component analysis. B, Gene Ontology (GO) analysis of biological processes differentially affected by the *flk* mutations. These GO categories were significantly different in all four comparison groups: (a) Col-0 vs. *flk-1*; (b) Col-0 vs. *flk-5*; (c) *acd6-1* vs. *acd6-1 flk-1*; and (d) *acd6-1* vs. *acd6-1 flk-5*. C, Heatmap analysis of defense genes differentially affected by the *flk* mutations. D, Suppression of major defense genes by the *flk* mutations in *acd6-1*. The GO category for salicylic acid (SA) is GO:0009751 (response to SA), for jasmonic acid (JA) GO:0009753 (response to JA), for ethylene (ET) GO:0009723 (response to ET), for programmed cell death (PCD) GO:0008219 (cell death), and for PAMP-triggered immunity (PTI) GO:0007166 (cell surface receptor signaling pathway).

vs. *flk-1*; (b) Col-0 vs. *flk-5*; (c) *acd6-1* vs. *acd6-1 flk-1*; and (d) *acd6-1* vs. *acd6-1 flk-5* (Supplemental Dataset S2). There was an enrichment of genes involved in development and defense in the DAS genes (Supplemental Figure S3 and Supplemental Dataset S2). Among these DAS genes, 219 also showed differential expression influenced by the *flk* mutations (Supplemental Dataset S3).

One of the DAS genes identified in our bioinformatics analysis is *ACD6*. There are six major isoforms for the *ACD6* transcript, according to Arabidopsis Thaliana Reference Transcript Dataset 2 (Zhang et al., 2017) (Supplemental Figure S4A). DAS analysis indicated that the At4g14400_ID4 isoform, which includes the third intron, was significantly induced by the *flk* mutations in the *acd6-1* background (Figure 5A). We confirmed this result by RT-PCR, which showed a clear increase in the At4g14400_ID4 isoform in the *acd6-1 flk* mutants compared with in *acd6-1* (Supplemental Figure S4B, primer set 1). In addition, we detected an extra band with primer set 2, which flanked intron 4 of the gene, the level of which was higher in the *acd6-1 flk* mutants than in *acd6-1* (Supplemental Figure S4B, primer set 2). The size of this band is the same as the amplicon from the genomic DNA template, suggesting the retention of intron 4 due to the *flk* mutations. The

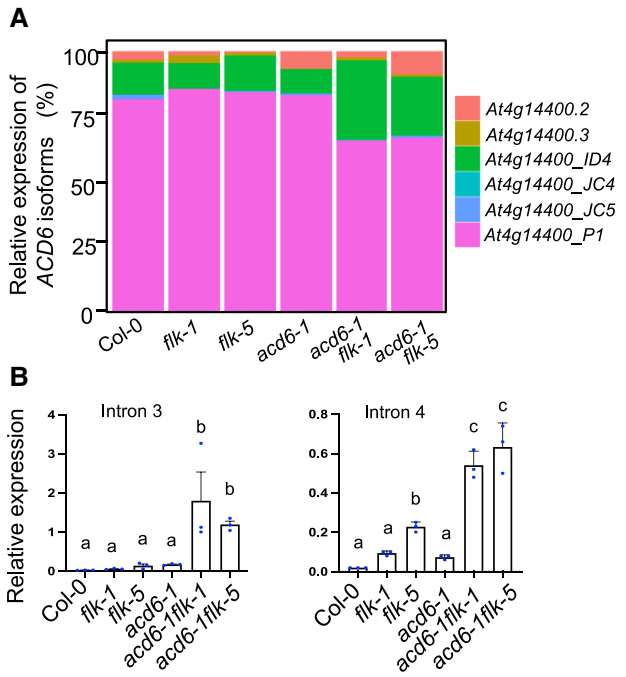

Figure 5 FLK regulates alternative splicing of *ACD6* transcripts. A, Relative abundance of *ACD6* isoforms in different genotypes from 3D RNA-seq analysis. Colors indicate six major isoforms of ACD6 transcript, according to Arabidopsis Thaliana Reference Transcript Dataset 2. B, RT-qPCR analysis of expression of intron 3 and intron 4 using intron specific primers. Error bars represent mean ± SEM ($n = 3$). Different letters indicate significant difference among the samples ($P < 0.05$; One-way ANOVA).

amplicons corresponding to intron 3 or intron 4 retention were further confirmed by sequencing. No difference in ACD6 isoforms was observed with primer sets 3 and 4 (Supplemental Figure S4B).

While it can aid the visualization of *ACD6* isoforms with different primer sets, RT-PCR is less reliable in accurately quantifying the abundance of specific isoforms. Therefore, we conducted RT-qPCR to measure the levels of intron-containing isoforms using intron specific primers (Supplemental Table S1). Figure 5B showed significantly higher levels of intron 3 and intron 4 expression in the *acd6-1 flk* mutants than in *acd6-1*. Retention of intron 3 and 4 in *acd6-1flk* mutants should result in early translation terminations (Supplemental Figure S5A). While the wild-type ACD6 protein is predicted to have nine ankyrin repeats and five transmembrane helix, the predicted ACD6 isoforms with intron 3 or with intron 4 are truncated and only have four and nine ankyrin repeats, respectively (Supplemental Figure S5B). Such protein truncates likely lead to reduced or null function of the encoded proteins.

We further observed that *ACD6* expression was much higher in the *acd6-1* background than in the Col-0 background (Supplemental Figure S2 and Supplemental Dataset S1), consistent with prior reports that demonstrated *acd6-1* is a hypermorphic allele (Lu et al., 2003). Interestingly, *ACD6* transcript abundance was comparable in *acd6-1 flk* mutants and *acd6-1* (Supplemental Figure S2 and Supplemental Dataset S1). Thus, increased retention of intron 3 and intron 4 will likely reduce the overall function of *ACD6* in the *acd6-1 flk* mutants, contributing to *flk* suppression of *acd6-1*-conferred phenotypes and defense. Together, these results lend strong support for the role of FLK in targeting *ACD6* for alternative splicing, accounting at least partly for FLK function in regulating defense and *acd6-1*-conferred phenotypes.

Multiple SA regulators contribute to the regulation of *acd6-1*-conferred phenotypes by FLK

In addition to the *flk* mutations, defects in a number of SA genes were previously reported to suppress *acd6-1*-conferred phenotypes (Ng et al., 2011; Wang et al., 2011a). Because our RNA-seq analysis showed that expression of several major SA genes, including two SA biosynthesis genes (*ICS1* and *WIN3*), an SA regulatory gene (*PAD4*), and an SA receptor gene (*NPR1*), was suppressed in the *acd6-1 flk* mutants, compared with in *acd6-1* (Figure 4D and Supplemental Data S1), we hypothesized that these SA genes act downstream of *FLK* to affect FLK-mediated defense and development. To test this hypothesis, we crossed the *flk-1* mutant with mutants impaired in these SA genes, including *ics1-1*, *win3-1*, *pad4-1*, and *npr1-1*, in the *acd6-1* background. Like *acd6-1 flk-1*, all the double mutants, *acd6-1 ics1-1*, *acd6-1 win3-1*, *acd6-1 pad4-1*, and *acd6-1 npr1-1*, are larger than *acd6-1* and showed reduced cell death relative to *acd6-1* (Figure 6, A and B and Ng et al., 2011; Wang et al., 2011a). We obtained higher-order mutant combinations and analyzed these plants for *acd6-1*-conferred phenotypes, including plant size, cell death, and SA level. We made inferences on the interactions of *FLK* and an SA gene on the basis of these phenotypes displayed by the higher-order mutants. A nonadditive suppression of these phenotypes would suggest that *FLK* and the SA gene act in the same pathway, whereas an additive suppression would suggest that *FLK* acts partially through or independently of the SA gene. Similar analyses have been successfully used to interrogate the genetic interactions among several defense genes (Song et al., 2004; Ng et al., 2011; Wang et al., 2011a; Wang et al., 2014; Hamdoun et al., 2016; Zhang et al., 2019).

For plant size and cell death, we found that all triple mutants containing *acd6-1* and *flk-1* showed much larger plant stature and reduced cell death than the corresponding double mutants (Figure 6, A and 6B). These results suggest that *FLK* acts partially through each of these SA pathway genes, *ICS1*, *PAD4*, *WIN3*, or *NPR1*, in regulating *acd6-1*-conferred dwarfism and cell death.

We further measured the total SA level in these plants (Figure 6C). Consistent with the roles of ICS1 and WIN3 as major SA synthesis proteins, there were residual SA levels in *acd6-1 ics1-1* and *acd6-1 win3-1* with or without the presence of *flk-1*. While *pad4-1* suppressed SA accumulation in

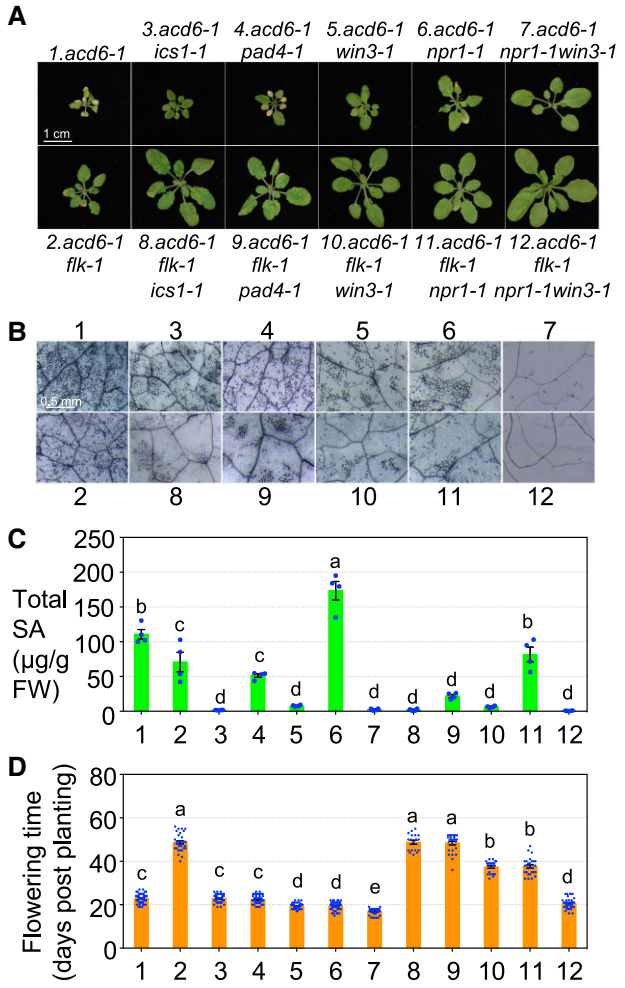

Figure 6 Genetic analysis of the interactions between *flk-1* and major SA mutants in *acd6-1*. A, Pictures of 25-d old plants. The size bar represents 1 cm and is applied to all panels. B, Cell death staining. The size bar represents 0.5 mm and is applied to all panels. C, Total salicylic acid (SA) measurement by HPLC. D, Flowering time. Plants were grown in a light cycle of 16 h L/8 h D and recorded for flowering time, days after planting for the first visible appearance of inflorescence of a plant. Error bars represent mean ± SEM in C, ($n = 4$) and D, ($n \geq 18$). Different letters indicate significant difference among the samples ($P < 0.05$; One-way ANOVA with post hoc Tukey's HSD test). Data for Col-0 and *flk-1* were shown in Figure 1. These experiments were repeated two times with similar results.

acd6-1, the SA receptor mutant *npr1-1* led to a high SA level in *acd6-1* (Figure 6C and Ng et al., 2011). Further reduced SA levels were found in *acd6-1 flk-1 pad4-1* and *acd6-1 flk-1 npr1-1* compared with in the corresponding double mutants, suggesting that FLK acts partially through PAD4 and NPR1 in SA regulation.

FLK regulation of flowering is largely independent of Sa

We were interested in elucidating how FLK-mediated flowering is related to its role in SA regulation. We quantified the flowering time under the same light condition (12 h light [L]/12 h dark [D]) used for SA measurement and other defense assays. Although they had drastic differences in SA levels, the *acd6-1 flk* double and *flk* single mutants showed similar late flowering phenotypes (Figure 1D). The late flowering of *acd6-1flk-1* was not affected when additional SA deficient mutants, *ics1-1* or *pad4-1*, were introduced (Figure 6, C and D). Thus, we concluded that FLK-mediated flowering regulation is largely independent of SA under a 12 h L/12 h D cycle. In fact, Col-0 and *acd6-1* flowered at a similar time although they accumulated drastically different levels of SA (Figure 1 and Wang et al., 2011a). Thus, we believe that the effect of SA on flowering time regulation is minor under our condition.

We previously showed that *npr1-1* and *win3-1* work additively to stimulate early flowering and suppress *acd6-1*-conferred phenotypes (Figure 6 and Wang et al., 2011a). Consistent with this observation, we found here that *npr1-1* and *win3-1* individually suppressed late flowering of *flk-1*. Together in the quadruple mutant *acd6-1 flk-1 npr1-1 win3-1*, they brought the flowering time to the wild-type level and completely suppressed *acd6-1*-conferred small stature, cell death, and high SA level (Figure 6). However, the early flowering of *npr1-1* is likely due to a second site mutation in the background (Dong XN, personal communication). Together, these results suggest that WIN3, NPR1, and an unknown protein(s) act downstream of FLK to contribute to the regulation of flowering in addition to *acd6-1*-conferred phenotypes, including SA accumulation, cell death, and plant size.

Discussion

The FLK protein is known as a positive regulator of flowering time. We report here a role of FLK in pathogen defense. Our data showed that loss of function in FLK conferred enhanced disease susceptibility to the biotroph *P. syringae* and enhanced disease resistance to the necrotroph *B. cinerea*. The RNA-seq analysis supports that FLK acts through regulating expression and alternative splicing of target genes in defense and development. One such FLK target gene is *ACD6*. Thus, this study provides mechanistic links of FLK function in regulating *acd6-1*-conferred phenotypes as well as plant defense and development.

FLK encodes a putative protein with three KH motifs. The KH motif is a highly conserved RNA binding motif found in proteins from diverse organisms. KH-domain proteins were shown to affect RNA metabolism, such as pre-mRNA processing and mRNA stability (Nicastro et al., 2015). Our RNA-seq analysis revealed that many genes involved in development and defense were differentially expressed in the *flk* mutants compared with in control plants (Figure 4). In addition, the *flk* mutations affected alternative splicing of some gene transcripts, including *ACD6*. These observations support the biochemical function of FLK in affecting gene transcript levels as well as pre-mRNA processing.

We previously reported that *acd6-1* harbored a point mutation, causing a Leu-to-Phe substitution at position 591 of the ACD6 protein in a predicted transmembrane helix (Lu et al., 2003, 2005). This mutation makes ACD6-1 a gain-of-function and hypermorphic protein. Because *acd6-1* expresses high levels of *ACD6-1* and other defense genes and displays drastic defense-associated phenotypes as well as extreme dwarfism, *acd6-1* provides a sensitive background to detect the changes in gene expression and physiological phenotypes, which may not be otherwise detected in the Col-0 background. Indeed, our data showed that a lack of *FLK* expression led to increased retention of intron 3 and 4 in *ACD6* transcripts in the *acd6-1* background, however, there was less of such an increase in the Col-0 background (Figure 5). *ACD6-1* transcripts containing intron 3 and/or intron 4 should have translation terminations before the transmembrane domain (Supplemental Figure S5), likely leading to reduced or null function of the encoded proteins. Therefore, although the abundance of *ACD6-1* transcripts remains similarly high in *acd6-1* and *acd6-1 flk* mutants (Supplemental Figure S2 and Supplemental Dataset S1), the increased amount of aberrant splicing of *ACD6* transcripts in *acd6-1 flk* mutants could drastically reduce the function of ACD6-1, leading to a partial suppression of *acd6-1*-conferred phenotypes by the *flk* mutations.

Suppression of *acd6-1*-conferred phenotypes by *flk* could also be due to FLK regulation of other defense genes. Indeed, our RNA-seq analysis showed that FLK influenced expression of a large number of defense genes, including those involved in SA, JA, ET, PCD, and PTI. In particular, a number of major SA pathway genes involved in SA biosynthesis, SA regulation, and SA perception were down-regulated in the *acd6-1 flk* mutants than in *acd6-1* (Figure 4D and Supplemental Data S1). Because *acd6-1*-conferred phenotypes are sensitized to changes in SA levels and/or signaling, such lower expression of the SA pathway genes could also contribute to the partial suppression of *acd6-1*-conferred dwarfism, cell death, and high SA accumulation in the *flk* mutant, in addition to the influence of FLK on *ACD6* alternative splicing. Consistent with multiple downstream defense targets of FLK, our genetic analysis showed that FLK acts only partially through each of the SA pathway genes, *ICS1*, *PAD4*, *WIN3*, and/or *NPR1*, in influencing *acd6-1*-conferred plant size and cell death (Figure 6). While requiring the major SA biosynthesis genes *ICS1* and *WIN3* for SA accumulation, FLK-mediated SA accumulation is partially through the known SA regulator PAD4. These data further suggest that expression of these SA genes is likely regulated by additional factors in addition to FLK. This is because the full effect of these genes can only be detected when they are completely knocked out, leading to enhanced *flk* suppression of *acd6-1*-conferred phenotypes (Figure 6).

Consistent with FLK regulation of *ACD6*, SA regulatory genes, and those involved in additional defense signaling pathways, the *flk* mutations resulted in lower resistance to the biotroph *PmaDG3* and suppressed SA accumulation induced by *PmaDG3* infection (Figures 1 and 2). While S, A is a key signaling molecule critical for defense against biotrophs, SA could adversely affect plant resistance against necrotrophs through cross-talking with other defense pathways, such as those mediated by JA. Indeed, our data showed an increased resistance of the *flk* mutants to the necrotrophic pathogen *B. cinerea*, associating with decreased expression of JA signaling repressor genes and increased expression of the JA signaling marker gene *PDF1.2* compared with expression in Col-0 (Figure 3 and Supplemental Figure S2). Thus, our data support the crosstalk between SA and JA signaling.

Previous studies showed a positive role of SA in influencing flowering time. Plants with lower SA levels, the *NahG* transgenic plant or the SA mutants *ics1* and *eds5*, flowered later than Col-0 (Martinez et al., 2004). It is worth noting that the effect of SA deficiency on flowering time in these plants appeared to be more evident in a short-day photoperiodic condition of 8 h L and 16 h D. In congruent with our defense assays, which were conducted under 12 h L or 16 h L in a 24 h cycle, we quantified flowering time with the same light regime. Under these conditions, we found that Col-0 and *acd6-1* had similar flowering time although there was a drastic difference in the SA levels. Thus, we believe that the effect of SA on flowering time regulation is minor with 12 h or more L in a day (Figures 1D and 6D and Wang et al., 2011a). Consistent with this note, our additional data failed to reveal a strong association of SA levels and FLK-mediated flowering regulation. For instance, these plant pairs, e.g. *acd6-1 flk-1/-5* vs. *flk-1/-5* and *acd6-1 flk-1* vs. *acd6-1 ics1-1 flk-1*, had large differences in SA levels yet they all showed *flk*-like late flowering (Figures 1 and 6). Thus, we concluded that, FLK-mediated flowering regulation is largely independent of SA under our experimental conditions. However, we do not exclude the possibility that the effect of SA mutants on *flk*-conferred late flowering could be detected under different light conditions, e.g. 8 h L/16 h D cycle, or with different light intensities. Because we are interested in FLK's role in regulating development and defense, flowering time quantification under a different light condition would require additional experiments to test the defense role of FLK under the same condition, e.g. FLK's regulation of SA accumulation and pathogen infections.

Of the SA mutants we tested, only *npr1-1* and *win3-1* showed contributions to FLK's role in flowering regulation. Because the flowering phenotype in the *npr1-1* mutant is likely due to a second site mutation, a further identification of this mutation should shed light on the molecular pathway(s) mediated by FLK in flowering control. *WIN3* encodes a GH3 acyl adenylase-family enzyme that conjugates glutamate to isochorismate to produce isochorismate-9-glutamate, a precursor of SA (Rekhter et al., 2019; Torrens-Spence et al., 2019). The lack of WIN3 enzymatic activity might produce an altered metabolic profile; one or more such metabolites could contribute to altered defense and flowering in the *win3-1* mutant. Our previous data suggest that these two roles of WIN3 are independent of each other (Wang et al., 2011a). WIN3 suppresses expression of

the flowering activator gene *FT* and promotes the repressor gene *FLC*. This action of WIN3 is opposite to that of FLK in regulating expression of these two genes (Lim et al., 2004; Mockler et al., 2004), likely forming the basis of *win3* suppression of *flk* in flowering control.

How does FLK execute its function in regulating various downstream pathways to affect defense and development of plants? The KH-domain proteins can function through a direct binding to and/or an association in protein complexes with RNA molecules for processing (Nicastro et al., 2015). It is possible that FLK directly binds to its target gene transcripts to influence their mRNA stability and/or alternative splicing. Alternatively, FLK could form protein complexes with other proteins to regulate pre-mRNA processing. Indeed, the FLK protein was previously shown to physically interact with several proteins, including three RNA binding proteins (PEPPER 1, HUA ENHANCER 4, and HUA1) (Cheng et al., 2003; Ripoll et al., 2009; Rodriguez-Cazorla et al., 2015), and an E3 ubiquitin ligase (HIGH EXPRESSION OF OSMOTICALLY RESPONSIVE GENES 1) (Lee et al., 2012). A recent study further showed that FLK and some of the FLK interactor proteins were copurified with another flowering regulator FPA (Parker et al., 2021), suggesting that these proteins might form protein complexes. The FLK interactor proteins, PEP1, HEN4, and HUA1, were shown to be involved in alternative splicing of certain target genes (Ripoll et al., 2009; Hornyik et al., 2010). Although not known to affect alternative splicing of gene transcripts, FPA was demonstrated to have a role in promoting 3′ end poly(A) site selection of gene transcripts in Arabidopsis (Parker et al., 2021). However, none of these FLK-associated RNA binding proteins have been shown to directly bind to their potential transcript targets. More research will be necessary to reveal direct transcriptional regulation of target genes of FLK and its associated proteins, filling this knowledge gap.

While the detailed biochemical mechanism by which FLK acts to regulate RNA metabolism remains to be elucidated, this report strongly supports the multifunctionality of FLK. It is possible that FLK multifunctionality is through its interaction with distinct protein partners to target downstream genes for their RNA levels and/or pre-mRNA processing. Such a multifunctionality of FLK could be decoupled by various downstream genes with distinct roles in defense and/or development regulation. Thus, it is critically important to uncover direct gene targets of FLK to further advance our understanding of the mechanistic actions of FLK. Some FLK pathway genes are potentially powerful molecular tools that can be used to develop novel biotechnological strategies to precisely control crop traits, maximizing plant growth while maintaining proper responses to environmental assaults.

Materials and methods

Plant materials

Arabidopsis (*A. thaliana*) plants were grown in growth chambers with 180 µmol m^{-2} s^{-1} photon density, 60% humidity, and 22°C, and a photoperiod of 12 h L/12 h D unless otherwise indicated. The *acd6-1 flk-5* mutant was isolated from the *acd6-1* suppressor screen (Lu et al., 2009) and was backcrossed to Col-0 to generate the *flk-5* mutant. The *flk-1* mutant (SALK_007750) was previously described (Mockler et al., 2004). The *acd6-1 flk-1* mutant was generated by crossing the two single mutants and selecting the homozygous double mutant in the F_2 generation, using relevant primers. The triple mutants of *acd6-1* and *flk-1* in combination with SA mutants, including *ics1-1*, *pad4-1*, *npr1-1*, and *win3-1*, were created by crossing the relevant mutants together. The triple mutants *acd6-1 flk-1 npr1-1* and *acd6-1 flk-1 win3-1* were previously described (Wang et al., 2011a) and were used to generate the quadruple mutant *acd6-1 flk-1 npr1-1 win3-1*. Primers for mutant allele detection were previously described (Ng et al., 2011; Wang et al., 2011a) or are listed in Supplemental Table S1.

Generation of transgenic complementation lines

A 5.9-kb fragment consisting of 2.4 kb *FLK* promoter and the 3.5 kb full-length *FLK* genomic fragment was PCR amplified, using primers xz798s_FLKproNotIF (ggg ccc gcg gcc gcA AGT TTC CAA CAC CAA GAA GCC A) and xz801s_FLKnonstopSalI (ggg ccc gtc gac GTA ACC GTA GCC TGA GCT GTA). The fragment was cloned in the pGlobug vector (Zhang and Mount, 2009) in frame at the 3′ end with the reporter gene *GFP*. The *pFLK-FLK-GFP-NOS* fragment was subcloned into the binary vector pMLBart, using the Not I site. This construct was designated as *FLK-GFP* and was used to transform the *flk-1* mutant, using *Agrobacterium*-mediated plant transformation. *flk-1* was chosen because both *FLK-GFP* and *flk-5* carried the BASTA gene, preventing herbicide selection for the transformants. Homozygous transgenic plants that are independent transformants were obtained from the T_2 generation.

Pathogen infection

Pseudomonas syringae pv. *maculicola* ES4326 strain DG3 (PmaDG3) was used to infect plants as previously described (Zhang et al., 2013). The fourth to seventh leaves of 25-d old plants were infiltrated with a PmaDG3 solution, using a needleless syringe. Discs of infected leaves were produced with a biopsy puncher of 4 mm diameter, homogenized in 10 mM $MgSO_4$, and serially diluted. The dilutions were plated on King's Broth agar media with 50 mg L^{-1} kanamycin for bacterial growth at 30°C.

Botrytis cinerea strain BO5-10 was kindly provided by Tesfaye Mengiste (Purdue University). A *B. cinerea* solution of 2×10^5 spores mL^{-1} was evenly sprayed onto plants for infection. Plants were covered for disease symptom development. Disease symptoms of the fourth to seventh leaves of each plant were scored three days post infection with the 1–5 scale as described (Wang et al., 2011a): 1 = no lesion or small, rare lesions; 2 = lesions on 10%–30% of a leaf; 3 = lesions on 30%–750% of a leaf; 4 = lesions on 50%–70% of a leaf; 5 = lesions on over 70% of a leaf.

SA quantification

SA extraction and quantification were performed as previously described (Wang et al., 2011a). For pathogen-induced SA accumulation, the fourth to seventh leaves of 25-d old plants were infiltrated with 1×10^7 cfu mL^{-1} PmaDG3 and were harvested at the indicated times for total SA extraction. For non-infected plants, the whole plants were collected for total SA extraction.

Gene expression analyses

Total RNA was extracted from the fourth to seventh leaves of 25-d old plants using TRIzol reagent (Invitrogen) per the manufacturer's instructions. After the removal of genomic DNA, total RNA was reverse-transcribed, using a cDNA synthesis kit (ThermoFisher Scientific). Maxima SYBR Green/ROX qPCR Master Mix (ThermoFisher Scientific) was used for qPCR reactions. *PDF2* (AT1G13320) was used as an internal control for RT-qPCR experiments (Czechowski et al., 2005). Amplicons from RT-PCR were sampled at 30 cycles. DNA electrophoresis was used to separate PCR amplicons of *ACD6* isoforms. Primers for RT-qPCR and RT-PCR are listed in Supplemental Table S1.

Luminol assay

Leaf discs of 4 mm diameter were isolated from the fourth to seventh leaves of 25-d old plants and floated atop 100 µl sterile water in a 96-well plate. The plate was covered with tin foil and placed in a growth chamber overnight to measure the PAMP-elicited ROS burst and for 2 h for basal ROS measurement. A 100 µl solution containing 300 µM L-012 (Wako Chemicals USA Inc. Richmond, VA) in 10 mM MOPS buffer (pH 7.4) and 1 µM flg22 or 1 µM elf26 was added to replace sterile water in each well and luminescence was recorded immediately using a Modulus II Microplate Reader.

Cell death staining

Trypan blue staining was performed to visualize cell death as previously described (Ng et al., 2011). Briefly, the fourth to seventh leaves of 25-d old plants were harvested and boiled in lactophenol (phenol: glycerol: lactic acid: water = 1:1:1:1; v/v) containing 0.01% trypan blue for 2 min. The stained leaves were boiled in alcoholic lactophenol (95% ethanol: lactophenol = 2:1 [v/v]) for 2 min, rinsed in 50% ethanol (v/v) for 1 min, and finally cleared in 2.5 g/ml chloral hydrate for 2 min. At least six leaves of each genotype were stained and visualized with a Leica M80 stereomicroscope. Cell death images were captured with a Leica IC80 HD camera connected to the microscope.

Callose staining assay

The fourth to seventh leaves of 25-d old plants were infiltrated with 1 µM flg22 or sterile water. Leaves were harvested 24 h post infiltration and boiled in alcoholic lactophenol (2:1 95% ethanol: lactophenol [v/v]) for 2 min followed by rinsing in 50% ethanol (v/v) for 1 min. Cleared leaves were stained with aniline blue solution (0.01% aniline blue (w/v) in 150 mM phosphate buffer, pH 9.5) for 90 min in darkness. Callose deposition was visualized with a Leica M205FA fluorescence stereomicroscope and photographed with an Amscope CMOS digital camera.

Root growth inhibition assay

Sterilized seeds were plated on agar plates containing ½ MS media supplemented with 1% sucrose (w/v) (pH 5.7), stratified at 4° C for 2 days, and then transferred to a tissue culture chamber to grow for 4 days. Seedlings of relatively uniform size were transferred to a 24-well tissue culture plate with 1.5 ml 1 µM flg22, or sterile water. A minimum of four seedlings per genotype per treatment were measured for root length 4 days post treatment and imaged with a Canon camera.

Flowering time determination

Flowering time was determined by counting the number of days post planting until the appearance of the first flower bud in plants. The light cycles were either long-day (16 h L/8 h D) or short-day (12 h L/12 h D). All plants used in this study for flowering time determination showed similar germination time.

RNA-seq analysis

Total RNA was extracted from 25-d old Col-0, *flk-1*, *flk-5*, *acd6-1*, *acd6-1 flk-1*, and *acd6-1 flk-5* plants. A total amount of 1 µg RNA per sample was used to generate cDNA libraries, using NEBNext® UltraTM RNA Library Prep Kit for Illumina® (NEB, USA) following manufacturer's recommendations. Deep sequencing was performed using Illumina NovaSeq 6000 (Novogene Corporation Inc.). Triplicate biological samples were used for all genotypes except *acd6-1 flk-5*, which had duplicate samples because one sample failed to pass quality control. The samples were multiplexed and sequenced with the standard paired-end sequencing that has a read length of 150 bp per end and 20 M reads per end per sample. The raw reads in FASTQ format were filtered by removing reads containing adapters and reads of low quality and mapped to the Arabidopsis genome (TAIR 10). For global gene expression profiling, a relative expression value (Reads Per Kilobase of transcript per Million mapped reads [RPKM]) higher than 0.3 was used as the cutoff to include genes for further analyses. Each RPKM value was corrected by adding the number one and then was $\log_2$-transformed. Differentially expressed genes were identified in four comparison groups: (a) Col-0 vs. *flk-1*; (b) Col-0 vs. *flk-5*; (c) *acd6-1* vs. *acd6-1 flk-1*; and (d) *acd6-1* vs. *acd6-1 flk-5*, using the R package DESeq2 with default parameters (Anders and Huber, 2010). Genes with an adjusted *P*-value <0.05 found by DESeq2 were assigned as differentially expressed. Gene Ontology (GO) enrichment analysis of DEGs was implemented by the clusterProfiler R package, in which gene length bias was corrected. GO analysis was also independently verified, using the online tool PANTHER (Mi et al., 2019).

Graphical representation of gene expression correlation was analyzed, using heatmap.2 function. DEGs were further corroborated via an additional independent analysis, using the webtool 3D RNA-seq (Calixto et al., 2018; Guo et al., 2021).

3D RNA-seq was further used to analyze differential alternative splicing (DAS) profiles of genes affected by the *flk* mutations. For DAS genes, the $\log_2$ fold change (L_2FC) of each individual transcript was compared to the weighted average of L_2FCs (weights were based on their standard deviation) of all remaining transcripts in the same gene. A gene was considered a significant DAS gene in a contrast group if any of its transcripts had a Δ Percent Spliced (ΔPS) ratio ≥ 0.1 with an adjusted P-value < 0.05 (Calixto et al., 2018).

Statistical analyses

Statistical analyses were performed using Prism 8 (GraphPad Software, LLC.). Details of experimental design, the number of replicates, and data presentation were indicated in the relevant figure legends and Method section.

Accession numbers

Sequence data from this article can be found in the GenBank/EMBL data libraries under accession number GSE164424.

Supplemental data

The following materials are available in the online version of this article.

Supplemental Figure S1. Complementation of the *flk-1* mutant by *FLK-GFP*.

Supplemental Figure S2. Regulation of gene expression by FLK.

Supplemental Figure S3. GO analysis of FLK regulated DAS genes.

Supplemental Figure S4. FLK regulates alternative splicing of *ACD6* transcripts

Supplemental Figure S5. Retention of intron 3 and/or intron 4 likely result in premature termination of the encoded ACD6 protein.

Supplemental Table S1. Primers used in this report.

Supplemental Dataset S1. Genes differentially affected by the *flk* mutations.

Supplemental Dataset S2. DAS of genes affected by the *flk* mutations.

Supplemental Dataset S3. DAS and differential expression of genes affected by the *flk* mutations.

Acknowledgments

We thank the members in the Lu laboratory for their assistance in this work. We thank Drs. Gordon Simpson and Ashis Nandi for helpful discussions.

Funding

This work was partially supported by grants from National Science Foundation, NSF 1456140 to Hua Lu and 1923069 to Xiaoning Zhang and Hua Lu, UMBC Technology Catalyst Fund, and UMBC CENTRE Funding Initiative.

Conflict of interest statement. None declared.

References

Amasino R (2010) Seasonal and developmental timing of flowering. Plant J **61**(6): 1001–1013

Anders S, Huber W (2010) Differential expression analysis for sequence count data. Genome Biol **11**(10): R106

Asai T, Tena G, Plotnikova J, Willmann MR, Chiu WL, Gomez-Gomez L, Boller T, Ausubel FM, Sheen J (2002) MAP Kinase signalling cascade in Arabidopsis innate immunity. Nature **415**(6875): 977–983

Bari R, Jones JD (2009) Role of plant hormones in plant defence responses. Plant Mol Biol **69**(4): 473–488

Boller T, Felix G (2009) A renaissance of elicitors: perception of microbe-associated molecular patterns and danger signals by pattern-recognition receptors. Annu Rev Plant Biol **60**: 379–406

Bu Q, Jiang H, Li CB, Zhai Q, Zhang J, Wu X, Sun J, Xie Q, Li C (2008) Role of the *Arabidopsis thaliana* NAC transcription factors ANAC019 and ANAC055 in regulating jasmonic acid-signaled defense responses. Cell Res **18**(7): 756–767

Calixto CPG, Guo W, James AB, Tzioutziou NA, Entizne JC, Panter PE, Knight H, Nimmo HG, Zhang R, Brown JWS (2018) Rapid and dynamic alternative splicing impacts the Arabidopsis cold response transcriptome. Plant Cell **30**(7): 1424–1444

Campos ML, Kang JH, Howe GA (2014) Jasmonate-triggered plant immunity. J Chem Ecol **40**(7): 657–675

Chen T, Cui P, Chen H, Ali S, Zhang S, Xiong L (2013) A KH-domain RNA-binding protein interacts with FIERY2/CTD phosphatase-like 1 and splicing factors and is important for pre-mRNA splicing in Arabidopsis. PLoS Genet **9**(10): e1003875

Cheng Y, Kato N, Wang W, Li J, Chen X (2003) Two RNA binding proteins, HEN4 and HUA1, act in the processing of AGAMOUS pre-mRNA in *Arabidopsis thaliana*. Dev Cell **4**(1): 53–66

Czechowski T, Stitt M, Altmann T, Udvardi MK, Scheible WR (2005) Genome-wide identification and testing of superior reference genes for transcript normalization in Arabidopsis. Plant Physiol **139**(1): 5–17

Dodds PN, Rathjen JP (2010) Plant immunity: towards an integrated view of plant-pathogen interactions. Nat Rev Genet **11**(8): 539–548

Endo J, Takahashi W, Ikegami T, Beppu T, Tanaka O (2009) Induction of flowering by inducers of systemic acquired resistance in the Lemna plant. Biosci Biotechnol Biochem **73**(1): 183–185

Falk A, Feys BJ, Frost LN, Jones JD, Daniels MJ, Parker JE (1999) EDS1, An essential component of R gene-mediated disease resistance in Arabidopsis has homology to eukaryotic lipases. Proc Natl Acad Sci USA **96**(6): 3292–3297

Feys BJ, Moisan LJ, Newman MA, Parker JE (2001) Direct interaction between the Arabidopsis disease resistance signaling proteins, EDS1 and PAD4. EMBO J **20**(19): 5400–5411

Feys BJ, Wiermer M, Bhat RA, Moisan LJ, Medina-Escobar N, Neu C, Cabral A, Parker JE (2005) Arabidopsis SENESCENCE-ASSOCIATED GENE101 stabilizes and signals within an ENHANCED DISEASE SUSCEPTIBILITY1 complex in plant innate immunity. Plant Cell **17**(9): 2601–2613

Fu ZQ, Dong X (2013) Systemic acquired resistance: turning local infection into global defense. Annu Rev Plant Biol **64**: 839–863

Fu ZQ, Yan S, Saleh A, Wang W, Ruble J, Oka N, Mohan R, Spoel SH, Tada Y, Zheng N, et al. (2012) NPR3 And NPR4 are receptors for the immune signal salicylic acid in plants. Nature **486**(7402): 228–232

Genoud T, Buchala AJ, Chua NH, Metraux JP (2002) Phytochrome signalling modulates the SA-perceptive pathway in Arabidopsis. Plant J **31**(1): 87–95

Geuens T, Bouhy D, Timmerman V (2016) The hnRNP family: insights into their role in health and disease. Hum Genet **135**(8): 851–867

Glazebrook J (2005) Contrasting mechanisms of defense against biotrophic and necrotrophic pathogens. Annu Rev Phytopathol **43**: 205–227

Griebel T, Zeier J (2008) Light regulation and daytime dependency of inducible plant defenses in Arabidopsis: phytochrome signaling controls systemic acquired resistance rather than local defense. Plant Physiol **147**(2): 790–801

Guan Q, Wen C, Zeng H, Zhu J (2013) A KH domain-containing putative RNA-binding protein is critical for heat stress-responsive gene regulation and thermotolerance in Arabidopsis. Mol Plant **6**(2): 386–395

Guo W, Tzioutziou NA, Stephen G, Milne I, Calixto CP, Waugh R, Brown JWS, Zhang R (2021) 3D RNA-seq: a powerful and flexible tool for rapid and accurate differential expression and alternative splicing analysis of RNA-seq data for biologists. RNA Biol **18**(11): 1574–1587

Hamdoun S, Zhang C, Gill M, Kumar N, Churchman M, Larkin JC, Kwon A, Lu H (2016) Differential roles of two homologous cyclin-dependent kinase inhibitor genes in regulating cell cycle and innate immunity in Arabidopsis. Plant Physiol **170**(1): 515–527

Hofmann E, Pollmann S (2008) Molecular mechanism of enzymatic allene oxide cyclization in plants. Plant Physiol Biochem **46**(3): 302–308

Hornyik C, Terzi LC, Simpson GG (2010) The spen family protein FPA controls alternative cleavage and polyadenylation of RNA. Dev Cell **18**(2): 203–213

Hsu FC, Chou MY, Chou SJ, Li YR, Peng HP, Shih MC (2013) Submergence confers immunity mediated by the WRKY22 transcription factor in Arabidopsis. Plant Cell **25**(7): 2699–2713

Jin JB, Jin YH, Lee J, Miura K, Yoo CY, Kim WY, Van Oosten M, Hyun Y, Somers DE, Lee I, et al. (2008) The SUMO E3 ligase, AtSIZ1, regulates flowering by controlling a salicylic acid-mediated floral promotion pathway and through affects on FLC chromatin structure. Plant J **53**(3): 530–540

Karasov TL, Chae E, Herman JJ, Bergelson J (2017) Mechanisms to mitigate the trade-off between growth and defense. Plant Cell **29**(4): 666–680

Korves TM, Bergelson J (2003) A developmental response to pathogen infection in Arabidopsis. Plant Physiol **133**(1): 339–347

Kunze G, Zipfel C, Robatzek S, Niehaus K, Boller T, Felix G (2004) The N terminus of bacterial elongation factor Tu elicits innate immunity in Arabidopsis plants. Plant Cell **16**(12): 3496–3507

Lee JH, Kim JJ, Kim SH, Cho HJ, Kim J, Ahn JH (2012) The E3 ubiquitin ligase HOS1 regulates low ambient temperature-responsive flowering in *Arabidopsis thaliana*. Plant Cell Physiol **53**(10): 1802–1814

Lee MW, Lu H, Jung HW, Greenberg JT (2007) A key role for the Arabidopsis WIN3 protein in disease resistance triggered by *Pseudomonas syringae* that secrete AvrRpt2. Mol Plant Microbe Interact **20**(10): 1192–1200

Libault M, Wan J, Czechowski T, Udvardi M, Stacey G (2007) Identification of 118 Arabidopsis transcription factor and 30 ubiquitin-ligase genes responding to chitin, a plant-defense elicitor. Mol Plant Microbe Interact **20**(8): 900–911

Lim MH, Kim J, Kim YS, Chung KS, Seo YH, Lee I, Hong CB, Kim HJ, Park CM (2004) A new Arabidopsis gene, FLK, encodes an RNA binding protein with K homology motifs and regulates flowering time via FLOWERING LOCUS C. Plant Cell **16**(3): 731–740

Lin SS, Martin R, Mongrand S, Vandenabeele S, Chen KC, Jang IC, Chua NH (2008) RING1 E3 ligase localizes to plasma membrane lipid rafts to trigger FB1-induced programmed cell death in Arabidopsis. Plant J **56**(4): 550–561

Liu J, Li W, Ning Y, Shirsekar G, Cai Y, Wang X, Dai L, Wang Z, Liu W, Wang GL (2012) The U-box E3 ligase SPL11/PUB13 is a convergence point of defense and flowering signaling in plants. Plant Physiol **160**(1): 28–37

Liu YG, Mitsukawa N, Oosumi T, Whittier RF (1995) Efficient isolation and mapping of Arabidopsis thaliana T-DNA insert junctions by thermal asymmetric interlaced PCR. Plant J **8**(3): 457–463

Lorkovic ZJ, Barta A (2002) Genome analysis: RNA recognition motif (RRM) and K homology (KH) domain RNA-binding proteins from the flowering plant *Arabidopsis thaliana*. Nucleic Acids Res **30**(3): 623–635

Lu H, Liu Y, Greenberg JT (2005) Structure-function analysis of the plasma membrane-localized Arabidopsis defense component ACD6. Plant J **44**(5): 798–809

Lu H, McClung CR, Zhang C (2017) Tick tock: circadian regulation of plant innate immunity. Annu Rev Phytopathol **55**: 287–311

Lu H, Rate DN, Song JT, Greenberg JT (2003) ACD6, a novel ankyrin protein, is a regulator and an effector of salicylic acid signaling in the Arabidopsis defense response. Plant Cell **15**(10): 2408–2420

Lu H, Salimian S, Gamelin E, Wang G, Fedorowski J, LaCourse W, Greenberg JT (2009) Genetic analysis of acd6-1 reveals complex defense networks and leads to identification of novel defense genes in Arabidopsis. Plant J **58**(3): 401–412

Lyons R, Iwase A, Gansewig T, Sherstnev A, Duc C, Barton GJ, Hanada K, Higuchi-Takeuchi M, Matsui M, Sugimoto K, et al. (2013) The RNA-binding protein FPA regulates flg22-triggered defense responses and transcription factor activity by alternative polyadenylation. Sci Rep **3**: 2866

March-Diaz R, Garcia-Dominguez M, Lozano-Juste J, Leon J, Florencio FJ, Reyes JC (2008) Histone H2A.Z and homologues of components of the SWR1 complex are required to control immunity in Arabidopsis. Plant J **53**(3): 475–487

Martinez C, Pons E, Prats G, Leon J (2004) Salicylic acid regulates flowering time and links defence responses and reproductive development. Plant J **37**(2): 209–217

Mi H, Muruganujan A, Huang X, Ebert D, Mills C, Guo X, Thomas PD (2019) Protocol update for large-scale genome and gene function analysis with the PANTHER classification system (v.14.0). Nat Protoc **14**(3): 703–721

Mockler TC, Yu X, Shalitin D, Parikh D, Michael TP, Liou J, Huang J, Smith Z, Alonso JM, Ecker JR, et al. (2004) Regulation of flowering time in Arabidopsis by K homology domain proteins. Proc Natl Acad Sci USA **101**(34): 12759–12764

Ng G, Seabolt S, Zhang C, Salimian S, Watkins TA, Lu H (2011) Genetic dissection of salicylic acid-mediated defense signaling networks in Arabidopsis. Genetics **189**(3): 851–859

Nicastro G, Taylor IA, Ramos A (2015) KH-RNA interactions: back in the groove. Curr Opin Struct Biol **30**: 63–70

Ning Y, Liu W, Wang GL (2017) Balancing immunity and yield in crop plants. Trends Plant Sci **22**(12): 1069–1079

Ortuno-Miquel S, Rodriguez-Cazorla E, Zavala-Gonzalez EA, Martinez-Laborda A, Vera A (2019) Arabidopsis HUA ENHANCER 4 delays flowering by upregulating the MADS-box repressor genes FLC and MAF4. Sci Rep **9**(1): 1478

Parker MT, Knop K, Zacharaki V, Sherwood AV, Tome D, Yu X, Martin PG, Beynon J, Michaels SD, Barton GJ, et al. (2021) Widespread premature transcription termination of Arabidopsis thaliana NLR genes by the spen protein FPA. Elife **10**: e65537. https://doi.org/10.7554/eLife.65537

Rate DN, Cuenca JV, Bowman GR, Guttman DS, Greenberg JT (1999) The gain-of-function Arabidopsis *acd6* mutant reveals novel regulation and function of the salicylic acid signaling pathway in controlling cell death, defenses, and cell growth. Plant Cell **11**(9): 1695–1708

Rekhter D, Ludke D, Ding Y, Feussner K, Zienkiewicz K, Lipka V, Wiermer M, Zhang Y, Feussner I (2019) Isochorismate-derived biosynthesis of the plant stress hormone salicylic acid. Science **365**(6452): 498–502

Ripoll JJ, Rodriguez-Cazorla E, Gonzalez-Reig S, Andujar A, Alonso-Cantabrana H, Perez-Amador MA, Carbonell J, Martinez-Laborda A, Vera A (2009) Antagonistic interactions between Arabidopsis K-homology domain genes uncover PEPPER as a

positive regulator of the central floral repressor FLOWERING LOCUS C. Dev Biol **333**(2): 251–262

Roden LC, Ingle RA (2009) Lights, rhythms, infection: the role of light and the circadian clock in determining the outcome of plant-pathogen interactions. Plant Cell **21**(9): 2546–2552

Rodriguez-Cazorla E, Ripoll JJ, Andujar A, Bailey LJ, Martinez-Laborda A, Yanofsky MF, Vera A (2015) K-homology nuclear ribonucleoproteins regulate floral organ identity and determinacy in Arabidopsis. PLoS Genet **11**(2): e1004983

Schaller F, Biesgen C, Mussig C, Altmann T, Weiler EW (2000) 12-oxophytodienoate reductase 3 (OPR3) is the isoenzyme involved in jasmonate biosynthesis. Planta **210**(6): 979–984

Seltmann MA, Stingl NE, Lautenschlaeger JK, Krischke M, Mueller MJ, Berger S (2010) Differential impact of lipoxygenase 2 and jasmonates on natural and stress-induced senescence in Arabidopsis. Plant Physiol **152**(4): 1940–1950

Singh V, Roy S, Giri MK, Chaturvedi R, Chowdhury Z, Shah J, Nandi AK (2013) *Arabidopsis thaliana* FLOWERING LOCUS D is required for systemic acquired resistance. Mol Plant Microbe Interact **26**(9): 1079–1088

Song JT, Lu H, McDowell JM, Greenberg JT (2004) A key role for ALD1 in activation of local and systemic defenses in Arabidopsis. Plant J **40**(2): 200–212

Spoel SH, Dong X (2008) Making sense of hormone crosstalk during plant immune responses. Cell Host Microbe **3**(6): 348–351

Stintzi A, Browse J (2000) The Arabidopsis male-sterile mutant, opr3, lacks the 12-oxophytodienoic acid reductase required for jasmonate synthesis. Proc Natl Acad Sci U S A **97**(19): 10625–10630

Thatcher LF, Kamphuis LG, Hane JK, Onate-Sanchez L, Singh KB (2015) The Arabidopsis KH-domain RNA-binding protein ESR1 functions in components of jasmonate signalling, unlinking growth restraint and resistance to stress. PLoS One **10**(5): e0126978

Torrens-Spence MP, Bobokalonova A, Carballo V, Glinkerman CM, Pluskal T, Shen A, Weng JK (2019) PBS3 and EPS1 complete salicylic acid biosynthesis from isochorismate in Arabidopsis. Mol Plant **12**(12): 1577–1586

Toruno TY, Stergiopoulos I, Coaker G (2016) Plant-pathogen effectors: cellular probes interfering with plant defenses in spatial and temporal manners. Annu Rev Phytopathol **54**: 419–441

Vanholme B, Grunewald W, Bateman A, Kohchi T, Gheysen G (2007) The tify family previously known as ZIM. Trends Plant Sci **12**(6): 239–244

Vellosillo T, Martinez M, Lopez MA, Vicente J, Cascon T, Dolan L, Hamberg M, Castresana C (2007) Oxylipins produced by the 9-lipoxygenase pathway in Arabidopsis regulate lateral root development and defense responses through a specific signaling cascade. Plant Cell **19**(3): 831–846

Wada KC, Yamada M, Shiraya T, Takeno K (2009) Salicylic acid and the flowering gene FLOWERING LOCUS T homolog are involved in poor-nutrition stress-induced flowering of Pharbitis nil. J Plant Physiol **167**(6): 447–452

Wang GF, Seabolt S, Hamdoun S, Ng G, Park J, Lu H (2011a) Multiple roles of WIN3 in regulating disease resistance, cell death, and flowering time in Arabidopsis. Plant Physiol **156**(3): 1508–1519

Wang L, Tsuda K, Sato M, Cohen JD, Katagiri F, Glazebrook J (2009) Arabidopsis CaM binding protein CBP60g contributes to MAMP-induced SA accumulation and is involved in disease resistance against *Pseudomonas syringae*. PLoS Pathog **5**(2): e1000301

Wang L, Tsuda K, Truman W, Sato M, Nguyen le V, Katagiri F, Glazebrook J (2011b) CBP60g and SARD1 play partially redundant critical roles in salicylic acid signaling. Plant J **67**(6): 1029–1041

Wang G, Zhang C, Battle S, Lu H (2014) The phosphate transporter PHT4; 1 is a salicylic acid regulator likely controlled by the circadian clock protein CCA1. Front Plant Sci **5**

Wildermuth MC, Dewdney J, Wu G, Ausubel FM (2001) Isochorismate synthase is required to synthesize salicylic acid for plant defence. Nature **414**(6863): 562–565

Woloszynska M, Le Gall S, Neyt P, Boccardi TM, Grasser M, Langst G, Aesaert S, Coussens G, Dhondt S, Van De Slijke E, et al. (2019) Histone 2B monoubiquitination complex integrates transcript elongation with RNA processing at circadian clock and flowering regulators. Proc Natl Acad Sci USA **116**(16): 8060–8069

Wu Y, Zhang D, Chu JY, Boyle P, Wang Y, Brindle ID, De Luca V, Despres C (2012) The Arabidopsis NPR1 protein is a receptor for the plant defense hormone salicylic acid. Cell Rep **1**(6): 639–647

Yan S, Dong X (2014) Perception of the plant immune signal salicylic acid. Curr Opin Plant Biol **20C**: 64–68

Yan Z, Jia J, Yan X, Shi H, Han Y (2017) Arabidopsis KHZ1 and KHZ2, two novel non-tandem CCCH zinc-finger and K-homolog domain proteins, have redundant roles in the regulation of flowering and senescence. Plant Mol Biol **95**(6): 549–565

Zhang R, Calixto CPG, Marquez Y, Venhuizen P, Tzioutziou NA, Guo W, Spensley M, Entizne JC, Lewandowska D, Ten Have S, et al. (2017) A high quality Arabidopsis transcriptome for accurate transcript-level analysis of alternative splicing. Nucleic Acids Res **45**(9): 5061–5073

Zhang C, Frias MA, Mele A, Ruggiu M, Eom T, Marney CB, Wang H, Licatalosi DD, Fak JJ, Darnell RB (2010a) Integrative modeling defines the Nova splicing-regulatory network and its combinatorial controls. Science **329**(5990): 439–443

Zhang C, Gao M, Seitz NC, Angel W, Hallworth A, Wiratan L, Darwish O, Alkharouf N, Dawit T, Lin D, et al. (2019) LUX ARRHYTHMO mediates crosstalk between the circadian clock and defense in Arabidopsis. Nat Commun **10**(1): 2543

Zhang T, Huang XH, Dong L, Hu D, Ge C, Zhan YQ, Xu WX, Yu M, Li W, Wang X, et al. (2010b) PCBP-1 regulates alternative splicing of the CD44 gene and inhibits invasion in human hepatoma cell line HepG2 cells. Mol Cancer **9**: 72

Zhang XN, Mount SM (2009) Two alternatively spliced isoforms of the Arabidopsis SR45 protein have distinct roles during normal plant development. Plant Physiol **150**(3): 1450–1458

Zhang C, Xie Q, Anderson RG, Ng G, Seitz NC, Peterson T, McClung CR, McDowell JM, Kong D, Kwak JM, et al. (2013) Crosstalk between the circadian clock and innate immunity in Arabidopsis. PLoS Pathog **9**(6): e1003370

Zhang Y, Xu S, Ding P, Wang D, Cheng YT, He J, Gao M, Xu F, Li Y, Zhu Z, et al. (2010c) Control of salicylic acid synthesis and systemic acquired resistance by two members of a plant-specific family of transcription factors. Proc Natl Acad Sci USA **107**(42): 18220–18225

Zheng XY, Spivey NW, Zeng W, Liu PP, Fu ZQ, Klessig DF, He SY, Dong X (2012) Coronatine promotes *Pseudomonas syringae* virulence in plants by activating a signaling cascade that inhibits salicylic acid accumulation. Cell Host Microbe **11**(6): 587–596

Zipfel C, Robatzek S, Navarro L, Oakeley EJ, Jones JD, Felix G, Boller T (2004) Bacterial disease resistance in Arabidopsis through flagellin perception. Nature **428**(6984): 764–767